Hohendorff, Bernd; Weidermann, Christian; Pollinger, Philipp; Burkhart, Klaus J.; Müller, Lars Peter:

Jamming of fingers: an experimental study to determine force and deflection in participants and human cadaver specimens for development of a new bionic test device for validation of power-operated motor vehicle side door windows

Zuerst erschienen in:	Biomedical Engineering = Biomedizinische Technik. - Berlin [u.a.] : de Gruyter. - 58 (2013), 1, p. 39-49.
Erstveröffentlichung:	2012-12-02
ISSN (online):	1862-278X
ISSN (print):	0013-5585
DOI:	10.1515/bmt-2012-0004
[*Zuletzt gesehen:*	2019-07-18]

Bernd Hohendorff*, Christian Weidermann, Philipp Pollinger, Klaus J. Burkhart and Lars Peter Müller

Jamming of fingers: an experimental study to determine force and deflection in participants and human cadaver specimens for development of a new bionic test device for validation of power-operated motor vehicle side door windows

Abstract: The deformability of human fingers is central to addressing the real-life hazard of finger jamming between the window and seal entry of a power-operated motor vehicle side door window. The index and little fingers of the left hand of 109 participants and of 20 cadaver specimens were placed in a measurement setup. Participants progressively jammed their fingers at five different dorsal-palmar jam positions up to the maximum tolerable pain threshold, whereas the cadaver specimens were jammed up to the maximum possible deflection. Force-deflection curves were calculated corresponding to increasing deflection of the compressed tissue layers of the fingers. The average maximum force applied by the participants was 42 N to the index finger and 35 N to the little finger. In the cadaver fingers, the average of the maximum force applied was 1886 N for the index finger and 1833 N for the little finger. In 200 jam positions, 25 fractures were observed on radiographs; fractures occurred at an average force of 1485 N. These data assisted the development of a prototype of a bionic test device for more realistic validation of power-operated motor vehicle windows.

Keywords: Finger; force-deflection curve; jamming; power-operated window.

***Corresponding author: Bernd Hohendorff,** Elbe Clinic Stade Buxtehude, Department of Handsurgery, Aesthetics and Plastic Surgery, Bremervörder Straße 111, D-21682 Stade, Germany, Phone: +49-(0) 4141-97-2897, Fax: +49-(0) 4141-97-2917, E-mail: bernd.hohendorff@hotmail.com
Christian Weidermann: Ilmenau University of Technology, Faculty of Mechanical Engineering, Institute of Thermodynamics and Fluid Mechanics, Helmholtzring 1, D-98684 Ilmenau, Germany
Philipp Pollinger: University of Applied Sciences Coburg, Department of Mechanical Engineering, Automotive Technology and Management, Mechatronics, Friedrich-Streib-Straße 2, D-96450 Coburg, Germany
Klaus J. Burkhart and Lars Peter Müller: Department of Trauma, Hand and Elbow Surgery, Centre for Orthopaedic and Trauma Surgery, University Medical Center Cologne, Kerpener Straße 62, D-50937 Köln, Germany

Introduction

Modern motor vehicles are increasingly equipped with automatic power-operated windows with closing force restriction [2] in which a Hall sensor measures the speed of the window motor and registers resistance if the rotation frequency changes. The system must recognize within a few milliseconds whether there is an object caught between the window glass and the seal in a safety gap opening from 200 to 4 mm or whether there is merely stiffness in the guidance of the glass or another disturbance. This allows the closing of a window to be stopped immediately and the window to be lowered if an object is caught in the safety gap. Also, the window closing force should not exceed a limit of 100 N specified by various international guidelines [1, 9]. Closing force restriction systems are subject to legal requirements and must be validated with a test device. At present, closing force restriction is gauged at small dimensions using a simple steel rod with a 4-mm diameter, which is inserted in the gap between the window and seal entry during window validation. However, a small steel rod reproduces neither the variable diameter nor the elasticity of a human finger [6]. Additionally, no special test device exists for children's fingers, which are particularly at risk for serious injury in motor vehicle power windows.

In this experimental study, we first measured deflection and the corresponding force on participants' index and little fingers at five different dorsal-palmar jam positions up to the maximum tolerable pain threshold. Then, we measured deflection and force up to the maximum deflection and/or the respective point of fracture in human cadaver fingers. These data assisted the construction of a prototype of a bionic test device that closely reproduces and measures the real-life hazard, particularly for children, of finger jamming between the window and seal entry of a power-operated motor vehicle side door window.

Materials and methods

The girths of the proximal (PP), middle (MP), and distal (DP) phalanxes and of the proximal (PIP) and distal (DIP) interphalangeal joints of both the index and little fingers of the left hand of 109 participants (60 men, 49 women; median age, 33 years; range, 18–57 years) and of 20 cadaver hands (14 women, 6 men; median age, 81 years; range, 57–88 years) disarticulated at the wrist were measured using a measuring tape. Diameter was calculated from girth, which was assumed to be circular.

To measure finger deflection and corresponding force, a modified drilling-milling machine (Bohr Fräsmaschine Opti BF 20 Vario, Optimum Maschinen, Germany) was used, which was disconnected from the main voltage. A 4-mm-wide aluminum plate was bolted vertically to the hollow shaft and a corresponding aluminum plate was attached to the milling table in a bench vise. The shearing edges of the aluminum plates were rounded as in a normal motor vehicle side door window to avoid skin injuries. An electrometric path sensor (burster, type 8712-150, Gernsbach, Germany) and a subminiature force sensor (burster, type 8432-2000, Gernsbach, Germany) were connected to a computer (Dewetron, DEWE-5000, Grambach, Austria).

In the first part of the study, each participant placed his or her left hand, palm up, on the mounted bench vice with a finger placed in one of the five jam positions (Figure 1). Figure 2 shows the different finger jam positions: 1, flexion crease of the PP; 2, flexion crease of the PIP; 3, center of the MP; 4, flexion crease of the DIP; 5, center of the DP. Data recording was started on the computer. Using the star grip, each participant moved the shaft down with the right hand, jamming a finger between the two aluminum plates in order to reach his or her maximum tolerable pain threshold within 10 s. All participants gave informed consent, and the study was approved by the relevant Ethics Committee (Bavarian Ethics Committee) and conformed to the Declaration of Helsinki.

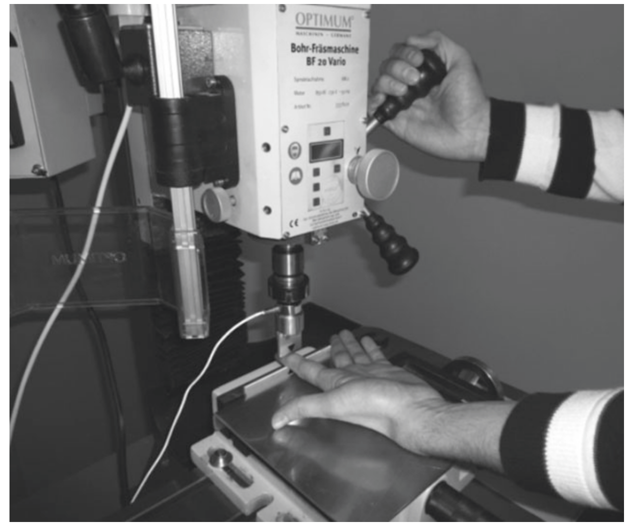

Figure 1 The participant moves the shaft down with the right hand by the star grip and jams his left index finger between the two aluminum sheets until the maximum subjectively tolerable pain level is reached.

In the second part of the study, the index and little fingers of the cadaver specimens were placed, palm up, on the mounted bench vice with a finger placed in one of the five jam positions corresponding to the participants' measurements. The index and little fingers in ten randomly chosen hands were jammed at the PP, MP, and DP,

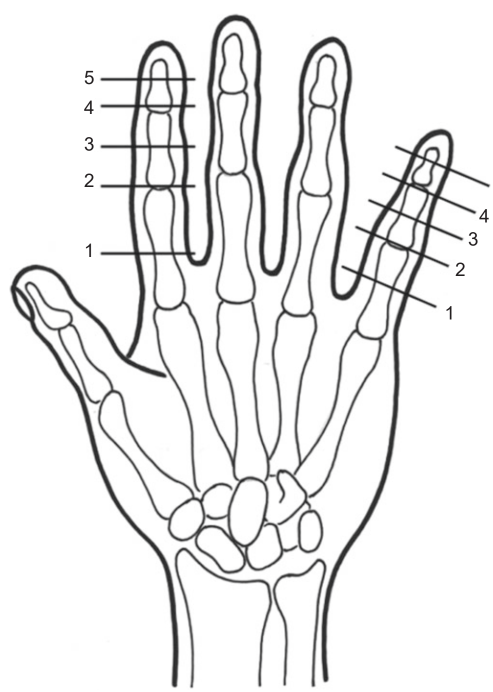

Figure 2 Five different finger jam positions: 1, flexion crease of the PP; 2, flexion crease of the PIP; 3, center of the MP; 4, flexion crease of the DIP; 5, center of the DP.

Table 1 Measured finger girth and calculated diameter of the index and little fingers (mean and standard deviation for participants and cadaver).

	Index finger					Little finger				
	Total (n=109)	Men (n=60)	Women (n=49)	Cadaver (n=20)	Test device	Total (n=109)	Men (n=60)	Women (n=49)	Cadaver (n=20)	Test device
Girth PP (mm)	69.2±6.1	69.3±6.3	69.1±6.0	67.8±7.8	50	58.6±5.5	58.7±5.7	58.5±5.4	56.2±5.5	42
Girth PIP (mm)	65.5±5.5	69.3±3.9	60.9±3.2	66.9±6.0	48	56.1±4.9	59.4±3.5	52.1±2.8	55.3±4.7	40
Girth MP (mm)	58.2±5.1	58.3±5.2	58.1±4.9	66.9±4.9	41	50.3±4.7	50.4±4.7	50.2±4.7	48.1±4.4	37
Girth DIP (mm)	54.8±4.7	57.9±3.6	50.9±2.7	54.1±5.0	36	47.8±4.5	50.8±3.4	44.1±2.5	46.3±4.6	34
Girth DP (mm)	49.6±4.3	49.6±4.6	49.5±4.6	46.5±4.0	33	43.6±4.4	43.6±4.4	43.6±4.4	40.9±4.4	29
Diameter PP (mm)	22.0±1.9	22.1±2.0	22.0±1.9	24.5±11.9	16	18.7±1.8	18.7±1.8	18.6±1.7	18.0±1.8	13
Diameter PIP (mm)	20.9±1.8	22.1±1.3	19.4±1.0	21.3±1.9	15	17.9±1.6	18.9±1.1	16.6±0.9	17.7±1.6	13
Diameter MP (mm)	18.5±1.6	18.6±1.7	18.5±1.6	18.0±1.6	13	16.0±1.5	16.0±1.5	16.0±1.5	15.4±1.5	12
Diameter DIP (mm)	17.4±1.5	18.4±1.1	16.2±0.9	17.6±1.5	12	15.2±1.4	16.2±1.1	14.0±0.8	14.9±1.5	11
Diameter DP (mm)	15.8±1.5	15.8±1.5	15.8±1.4	14.8±1.3	10	13.9±1.4	13.9±1.4	13.9±1.4	13.1±1.4	9

and in the other ten hands, at the PIP and DIP. One of us used the star grip and moved the shaft down within 10 s, jamming a finger between the two aluminum plates until reaching the maximum possible deflection. Radiographs in two standard planes were obtained of all cadaver fingers to detect fractures. Table 1 includes the average finger size measurements of participants and cadaver specimens.

Force and deflection values were sampled at a frequency of 100 Hz and the data were digitally recorded with software. Force-deflection curves were calculated from the data using the Matlab Ezyfit Toolbox (Matlab R2007b, MathWorks, MA, USA). Custom code was used to generate interpolated force-deflection curves of all participants and cadaver specimens. Due to the J-shaped curve progression, the power function ansatz $f(x)=a\times x^b+c$ was used for curve fitting, with the parameter c always equal to 0.

Using the data from participants and cadaver specimens, a prototype of a bionic test device was developed for more realistic validation of the hazard that automatic power-operated motor vehicle side door windows pose, particularly for the fingers of children (Figure 3). Ethical reasons rule out obtaining jam measurements from child participants, and child cadaver specimens are scarce. Therefore, we used adult participant and cadaver data for the production of a silicone hand with the dimensions of a 6-year-old child (Table 1), which were obtained in a previous study [2]. Inside each finger, pressure sensors were embedded in a special silicone mantle. The elastic properties of the silicone mantle were chosen in such a way as to accommodate a compression force of approximately 140 N, which approximates the 100 N statutory limit for closing force. The elastic properties of the silicone of the middle and ring fingers correspond to those of the index finger, assuming that the sizes are nearly equal.

In the third part of the study, the index and little fingers of the bionic test device were jammed at the five different jam positions in the same manner as described above; force and deflection values were sampled, and force-deflection curves were calculated.

To evaluate the prototype, data from the device and the participants were compared. Conformity of force-deflection curves of the bionic test device to those of participants was determined using confidence intervals from mean force values at 0.3-mm intervals of deflection at every jam position. Curves were in conformity where the force values at 0.3-mm intervals of deflection of the bionic test device fell within the respective 95% confidence intervals of mean force values at 0.3-mm intervals of deflection at every jam position. Cadaver and bionic test device force-deflection curves were not comparable due to the greater distances measured by the subminiature force sensor and the higher forces applied to the cadaver fingers.

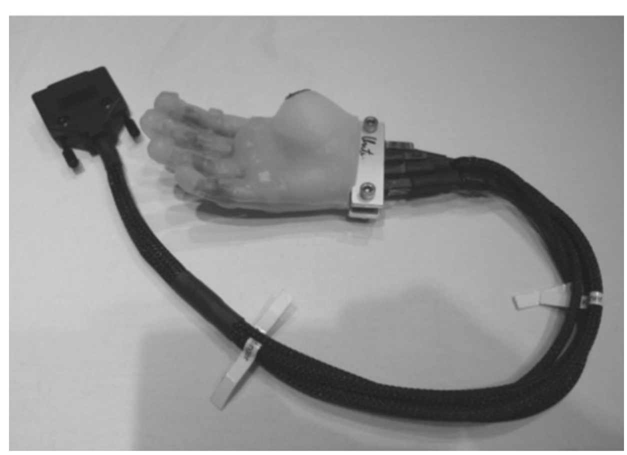

Figure 3 Bionic test device for more realistic validation of automatic power-operated motor vehicle side door windows.

Results

Table 2 shows the mean and standard deviation values of force and deflection at every jam position. The average maximum tolerable steadily applied force of the participants was 42 N for the index finger and 35 N for the little finger. No participant reported complications during and after finger jamming. In the cadaver specimens, the average maximum force was 1886 N for the index and 1833 N for the little finger. In 200 cadaver jam events, 25 fractures were observed on radiographs. Table 3 shows the distribution of the fractures and the respective force and deflection values at the point of fracture. Twenty-four fractures were observed at the phalangeal jam positions, one at an interphalangeal joint jam position. One index finger DP and one little finger DP were completely amputated. Fractures occurred at an average force of 1485 N.

All force-deflection curves showed J-shaped progression and represented increasing deformation across the compressed tissue layers of the finger. Figures 4A and 4B show raw data and corresponding interpolated force-deflection curves for participants' index and little fingers, respectively. Figures 5A and 5B show raw data and interpolated force-deflection curves of the PP, MP, and DP (Figure 5A) and the PIP and DIP (Figure 5B) of a cadaver (specimen no. 17) index finger. The arrows in Figure 5A point to the peaks of the raw data curves, which correspond to the points of fracture of the PP and MP. The DP of the index finger of this specimen did not break under maximum jamming force. The little peak at the end in curve 1 is due to inconstant force applied by the examiner upon bone compression. Fractures were not observed at jam positions PIP and DIP. The peaks at the ends of the curves in Figure 5B are also due to inconstant force applied by the examiner. Figures 6A and 6B show raw data and interpolated force-deflection curves of the PP, MP, and DP (Figure 6A) and the PIP and DIP (Figure 6B) of a cadaver specimen's little finger (specimen no. 18). The arrows in Figure 6A point to the peaks of the raw data curves, which correspond to the points of fracture of the PP, MP, and DP. Fractures were not observed at the PIP and DIP jam positions of the little finger of the specimen, which is confirmed by the J-shaped progression of the curves without a peak until maximum compression (Figure 6B).

Figures 7A and 7B show raw data and interpolated force-deflection curves of the bionic test device's index and little fingers. The J-shaped progression of the curves shows the continuous silicone compression. The incompressible metallic pressure sensor inside the silicone mantle accounts for the vertical slope at the curves' ends.

The size of the confidence intervals and, thereby, the variability of the participants' force-deflection curves increased with increasing deflection. Although the force-deflection curves of both the participants and bionic test device looked approximately the same, conformity by confidence intervals was only partial. At the DIP jam position of the index finger, force values of the bionic test device fell within the confidence intervals of the participants at two of eight points, and for the MP jam position, at five of 12 points of the measurement. No conformity was observed for the DP, PIP, and PP index finger jam positions. For the DP jam position of the little finger, force values of the bionic test device fell within participant confidence intervals at two of eight points; for the DIP jam position, at one of six points; and for the PIP jam position, at one of nine points of measurement. No

Table 2 Maximum force and deflection values at every jam position (mean and standard deviation for participants and cadaver).

	Participants (n=109)		Men (n=60)		Women (n=49)		Cadaver (n=20)		Test device	
	Force (N)	Deflection (mm)	Force (N)	Deflection (mm)	Force (N)	Deflection (mm)	Force (N)	Deflection (mm)	Force (N)	Deflection (mm)
Index finger										
PP	39.6±21.1	3.0±1.0	43.8±19.4	3.4±0.9	34.3±22.2	2.6±0.9	2068.6±469.3	19.6±2.0	143.9	10.2
PIP	44.6±20.3	2.6±0.9	49.8±20.7	2.8±0.8	38.0±17.9	2.3±0.6	1878.7±305.4	20.6±1.8	142.8	10.8
MP	48.8±22.9	3.6±1.1	56.7±22.7	4.0±1.1	39.0±19.3	3.1±0.9	2312.5±491.8	21.2±2.5	144.1	11.6
DIP	41.1±19.8	3.5±0.9	46.5±18.5	3.8±0.8	34.2±19.5	3.2±0.9	1494.3±185.5	23.0±0.3	143.6	10.1
DP	47.1±23.2	4.6±1.4	54.8±23.7	5.1±1.3	38.0±19.2	3.7±1.3	1674.7±460.5	23.0±2.8	141.1	12.6
Little finger										
PP	30.0±15.7	2.6±0.9	32.3±15.9	2.9±0.9	27.3±15.2	2.2±0.8	1702.3±688.7	19.0±6.4	144.1	10.5
PIP	35.6±16.3	2.1±0.8	39.4±16.0	2.3±0.9	30.7±15.6	1.8±0.6	1803.9±274.9	23.0±1.1	143.0	10.7
MP	39.1±17.4	2.9±0.9	43.6±17.1	3.1±0.9	33.4±16.2	2.5±0.8	1863.4±417.9	23.0±0.7	143.0	9.6
DIP	30.8±15.2	2.9±0.9	34.4±14.2	3.1±0.9	26.0±15.2	2.6±0.8	1939.5±331.5	23.2±0.8	144.3	14.9
DP	38.0±19.3	3.6±0.7	42.7±17.4	4.0±1.0	32.0±20.0	3.1±0.9	1855.2±361.1	24.1±0.3	144.3	14.9

Table 3 Fractures of cadaver specimens (force and deflection values at the point of onset of fracture).

Specimen no.	Jam position				
	PP	PIP	MP	DIP	DP
1	–	–	–	–	–
2	Index finger (1713 N; 23 mm)	–	Little finger (1821 N; 23 mm)	–	Index finger (1521 N; 23 mm)
3	–	–	–	–	–
4	–	–	–	–	Index finger (585 N; 18 mm) Little finger (467 N; 19 mm)
5	Index finger (1472 N; 13 mm)	–	–	–	Little finger (1328 N; 23 mm)
6	–	–	–	–	–
7	Index finger (2129 N; 15 mm)	–	Little finger (1244 N; 21 mm)	–	Little finger (2083 N; 24 mm)
8	–	–	–	–	–
9	–	–	–	–	Index finger, amputated (1716 N; 24 mm)
10	–	–	–	–	–
11	–	–	Index finger (474 N; 17 mm)	–	–
12	–	–	Little finger (291 N; 18 mm)	–	Index finger (1430 N; 23 mm)
13	–	–	–	–	–
14	Little finger (1489 N; 18 mm)		Little finger (2024 N; 23 mm)		Little finger (1898 N; 25 mm)
15	–	–	–	–	Index finger (1011 N; 22 mm) Little finger, amputated (1613 N; 24 mm)
16	–	–	–	–	–
17	Index finger (2090 N; 19 mm) Little finger (1247 N; 20 mm)		Index finger (2355 N; 21 mm) Little finger (1926 N; 22 mm)		Little finger (1426 N; 23 mm)
18	–	–	–	–	–
19	–	–	–	–	–
20	–	–	Little finger (1931 N; 22 mm)	–	Index finger (708 N; 20 mm) Little finger (1375 N; 23 mm)

N, Newton.

conformity of the bionic test device was observed for the MP and PP jam positions.

Discussion

This study is the first experimental investigation generating force-deflection curves of human fingers up to the subjective maximum tolerable pain threshold of participants and, similarly, of cadaver fingers – both undertaken to develop a prototype of a bionic test device to closely reproduce and measure the real-life situation of finger jamming between window and seal entry of a power-operated motor vehicle side door window. The force-deflection curves obtained in the dorsal-palmar direction at five different jam positions of the index and little fingers display characteristic nonlinearity, the increasing slope of which corresponds to increasing deformation across three compressed major layers or elastic elements of the finger: skin and subcutaneous fat, tendons, and bone or joint. While fractures that correspond to a severe finger jamming injury were observed at an average force of 1485 N in cadavers, and only 25 fractures were observed in 200 jam events, one fracture occurred at a force as low as 467 N, and we emphasize that serious finger injuries – even if they are not fractures – could occur above the subjective maximum tolerable pain threshold but below the 100 N closing force limit for power-operated windows. In January 2009, the National Highway Traffic Safety Administration in the US reported around 2000 injuries and five fatalities caused by automatic power-operated window systems [10]. Since 2005, the National Consumer Affairs Center in Japan has documented 23 finger injuries caused by the closure of power windows in motor vehicles [8]. Upon closing, a force of up to 500 N (corresponding to a weight of 50 kg) can be generated by the electric motor of the window lifter. Children are particularly at risk for serious injury in motor vehicle power windows due to seal designs [6] that allow a larger actual gap than the minimum statutory distance of 4 mm specified by the European guideline 74/60/EWG at which closing force restriction is disengaged. The need for more realistic validation of automatic power-operated motor vehicle side door windows thus motivated our development of a prototype of a new bionic test device that closely reproduces and measures real-life hazard, particularly for children. The dimensions of the device are those of an average 6-year-old child's fingers. At an average of 70% of the size of adult fingers, these dimensions approximate those of an adult closely enough that adult data could assist the design of the device.

Kent et al. [7] measured force and displacement tolerances for pinch loading of the bones and joints of human digits. Dynamic (54 mm/s) pinch loading was applied in a dorsal-palmar direction to all digits on matched pairs of hands from eight adult human cadavers. Opposed 3.1-mm-thick, 1.0-mm radius of curvature aluminum pinching surfaces were used to represent the geometry of moving surfaces in an automobile such as doors, lift gates, or window edges. Injury timing was determined

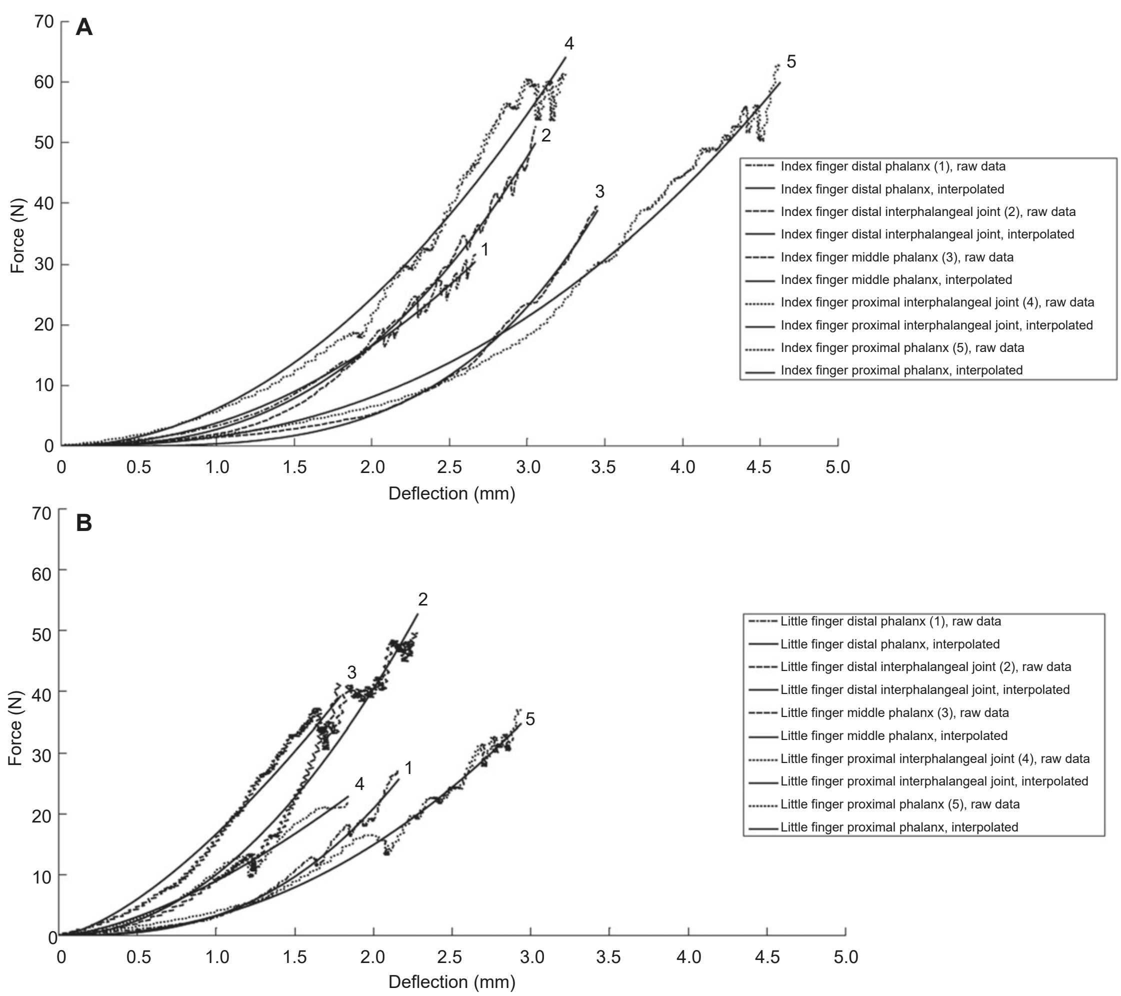

Figure 4 (A) Force-deflection curves from raw data and interpolated force-deflection curves of a participant's index finger. (B) Force-deflection curves from raw data and interpolated force-deflection curves of a participant's little finger.

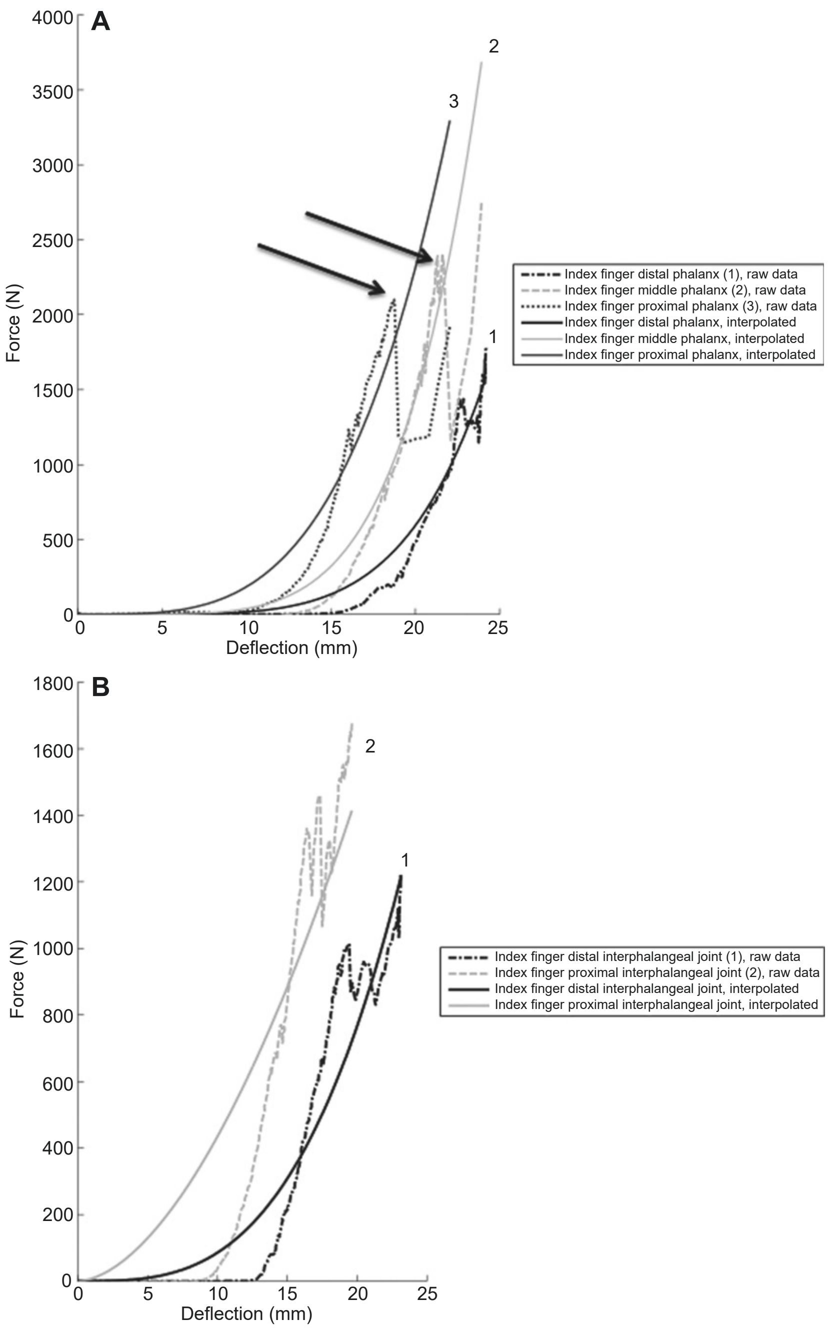

Figure 5 (A) Force-deflection curves from raw data and the respective interpolated force-deflection curves of the PP, MP, and DP of the index finger of specimen 17. The arrows point to the peaks of the raw data curves, which correspond to the points of fracture of the PP and MP. (B) Force-deflection curves from raw data and the respective interpolated force-deflection curves of the PIP and DIP of the index finger of specimen 17.

using acoustic sensors. The applied force and the distance between the pinching surfaces at the time of an acoustic burst were recorded. The force tolerance ranged from 245 N for the DP of the little finger to 1155 N for the MP of the index finger, with a general trend toward increasing force tolerance for more proximal anatomical structures. The distance between pinching surfaces (gap) at the time of injury ranged from 4.5 mm for the DIP joint of the little finger to 9.1 mm for the PP of the middle finger. Tuft fractures, transverse fractures, cortical crush injuries, a longitudinal fracture, and tendon injuries were observed. The authors stated that a value of approximately 35% of the initial dorsal-palmar dimension of the phalanx is reasonably representative of the gap tolerance for all digits

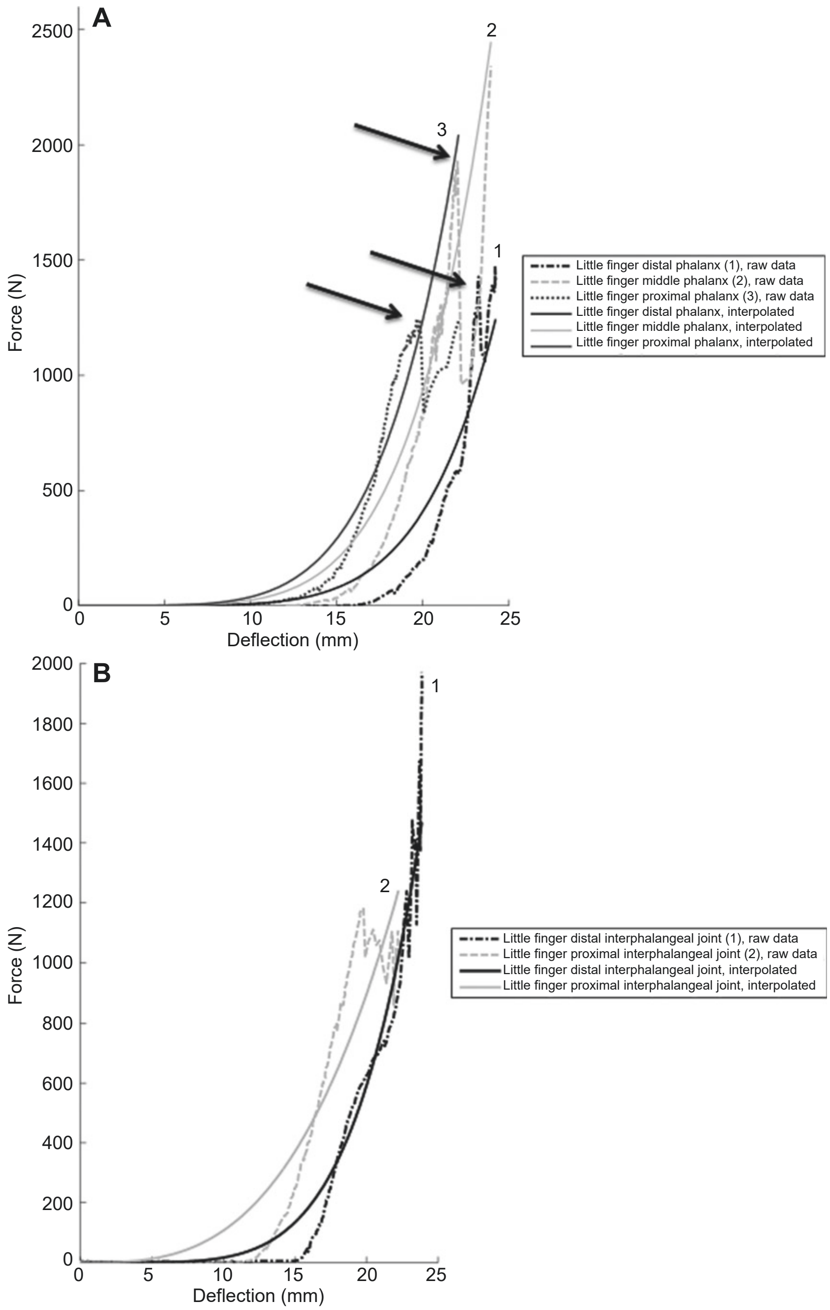

Figure 6 (A) Force-deflection curves from raw data and the respective interpolated force-deflection curves of the PP, MP, and DP of the little finger of specimen 18. The arrows point to the peaks of the raw data curves, which correspond to the points of fracture of the PP, MP, and DP. (B) Force-deflection curves from raw data and the respective interpolated force-deflection curves of the PIP and DIP of the little finger of specimen 18.

and loading sites. The tests would indicate that moving surfaces with geometry used in their study would not be expected to injure a digit if the opposing surfaces come no closer together than 35% of the digit's dorsal-palmar dimension.

Paridon and Mauser [11] studied deformability up to the subjective pain threshold of the index, middle, and ring fingers at the middle of the phalanxes and the knucklebones of 12 participants using a caliper gauge. The authors found the highest deformability at the lower phalanx and the lowest at the knucklebone. In our study, the highest deflection occurred for both the index and little fingers at the DP, whereas the smallest deflection was observed at the PIP of both fingers.

In a previous study of ours with the same 109 volunteers who participated in this study, we determined entrapment

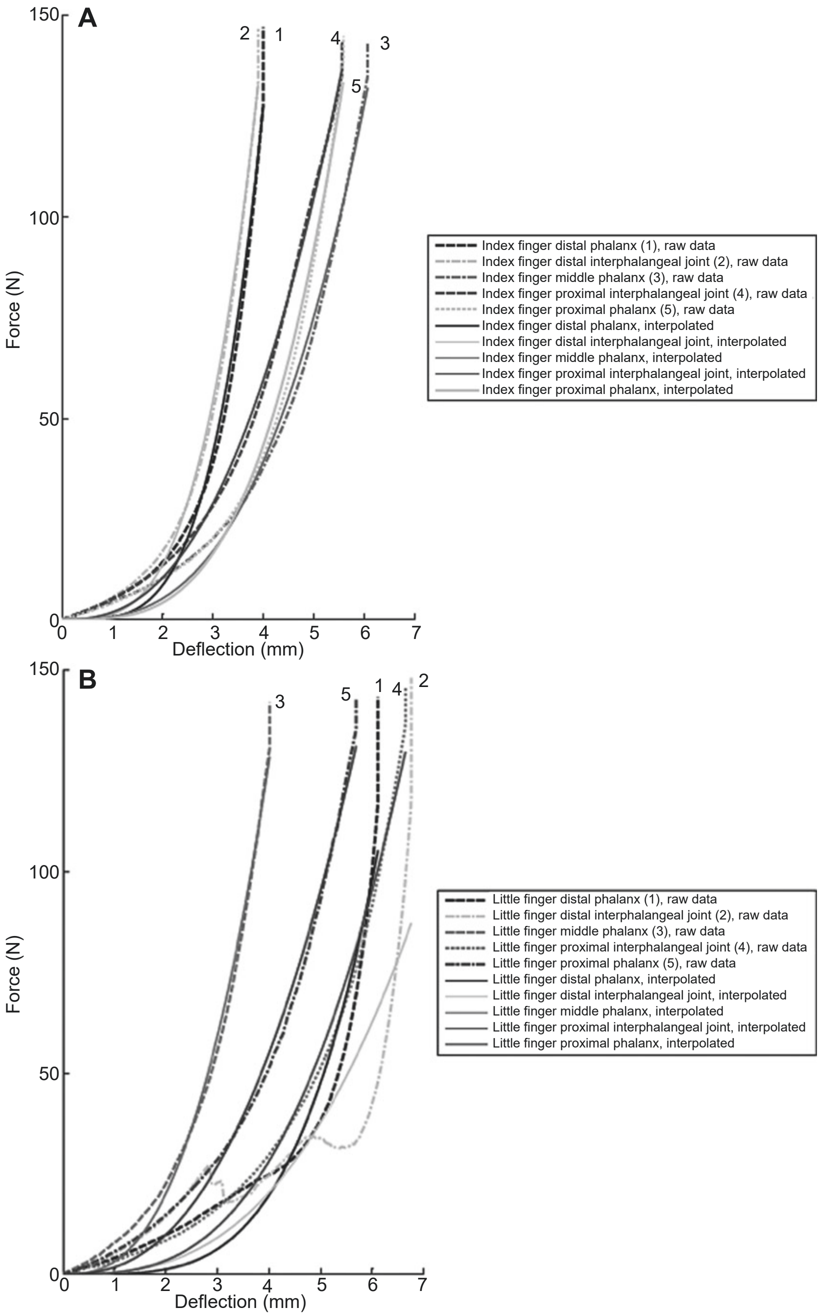

Figure 7 (A) Force-deflection curves from raw data and the respective interpolated force-deflection curves of the bionic test device's index finger. (B) Force-deflection curves from raw data and the respective interpolated force-deflection curves of the bionic test device's little finger.

forces acting on the participants' fingers at the subjective maximum pain threshold during entrapment between the window glass and seal entry of a motor vehicle side door [3]. The maximum bearable entrapment force was 97.2 N for the PIP of all triphalangeal fingers, 43.4 N for the index PIP, and 36.9 N for the index DIP. A positive correlation between finger diameter and maximum entrapment force was observed. Experimental determination of the point of onset of real finger injury in a jam event is obviously not possible.

In another previous investigation, we studied hands from 10 female cadaver specimens, which were disarticulated at the wrist and fixed in a special jig on the inside of a current motor vehicle side door [4]. Three different hand positions chosen to simulate real events in which a finger is jammed between the glass and seal entry of the window of a current motor vehicle side door were examined. The index, middle, ring, and little fingers of each hand were separately jammed both at the PIP and DIP at closing forces of 300 and 500 N with a constant window glass closing speed of 10 cm/s. These forces and the closing speed are representative of those of current motor vehicles. At 300 N, contusion marks of the skin, palmar joint instabilities, and superficial skin lesions occurred, whereas at 500 N, superficial skin lesions, superficial and deep open crush injuries, and fractures were observed.

In the current study, we observed fractures upon jamming at an average of 1485 N. The lowest force at the point of fracture was 467 N. The force applied to the cadaver phalanges and joints was a point load, whereas in our previous cadaver study [4], bending forces caused fractures at 500 N closing force with a constant window glass closing speed of 10 cm/s. These results do not exclude the possibility that finger lesions such as neurapraxia of the digital nerves or lymphedema could occur at a significantly lower closing force. Additionally, we are confident that children are particularly at risk of severe finger injuries at a lower closing force.

A further study we conducted emphasizes this point. Although ethical considerations rule out experimental study of children, we were able to determine the elastic resistance and the point of onset of bone/joint deformation at each of five different jam positions of an unembalmed finger that recently had been surgically removed from an 8-month-old polydactyl girl's finger [5]. The mean force at the point of onset of bone/joint deformation was 78.4 N. If a bone/joint deformation of a child's finger occurs at 70–80 N during jamming, which corresponds to a severe injury, it can be assumed that in a real jam event, soft tissue injuries could occur with significantly less closing force.

Our study has several limitations. Understandably, neither living children nor child cadavers are available for measurements such as those described in this study. Nevertheless, the risk that current power-operated window designs present to children is sufficiently high that it compels the use of relevant data available from adults. The subjective pain threshold of the adult participants showed large variance, one contributor to which may have been participant anxiety. Furthermore, it is possible that pain adaptation could have occurred during consecutive finger jamming at different jam positions, which also might have influenced our results. Although the fingertip has the highest density of sensory nerve endings, the participants applied less force at the PP and the DIP than at the fingertip. It is possible that the fingertip is less sensitive to pain due to pain adaptation to daily stress. But we certainly cannot explain why the participants applied more force at the DP than at the PP and DIP. We did not consider time dependence. Although each participant was instructed to reach his or her maximum tolerable pain threshold at each jam position within 10 s, the duration of jamming was not otherwise documented. It is possible that a fixed rate of force application during finger jamming might have led to different force-deflection curves, but we do not expect that such curves would differ markedly from the more experimentally (and ethically) feasible procedure in which participants were allowed to move the star grip of the modified drilling-milling machine by themselves. Finally, only cadaver specimens of the elderly were available. Whether different force-deflection curves would have resulted from younger specimens, especially those of children, could not be resolved. Age could have an impact on the incidence of fractures due to the relatively poorer bone quality of the elderly, in whom bone fracture is more probable than in the young, although we cannot explain why only 25 fractures occurred in 200 jam positions and why there were two amputations. It can be assumed that a fracture/amputation is related to the bone quality and thickness of the bone, but we did not find a correlation between fractures and dimensions of the fingers.

This prototype constitutes a promising first step toward the development of a test device that greatly improves upon the existing simple steel rod by allowing realistic simulation of the behavior of a real hand in the validation of automatic power windows. We are working on further improvement of bionic test devices to better assess and reduce the risk of jamming injuries, particularly to children, posed by power-operated windows.

Conflict of interest statement: Each author acknowledges having neither financial nor personal relationships with persons or organizations that would inappropriately influence this work.

Received August 16, 2012; accepted November 26, 2012; online first December 12, 2012

References

[1] Amtsblatt der Europäischen Gemeinschaft. Änderung der Richtlinie 74/60/EWG des Rates zur Angleichung der Rechtsvorschriften der Mitgliedstaaten über die Innenausstattung der Kraftfahrzeuge. 2000. L87/22.

[2] Hohendorff B, Weidermann C, Burkhart KJ, Rommens PM, Prommersberger KJ, Konerding MA. Lengths, girths, and diameters of child fingers from the age of 3 to 10 years. Ann Anat 2010; 192: 156–161.

[3] Hohendorff B, Weidermann C, Pollinger P, et al. Entrapment of adult fingers between window glass and seal entry of a motor vehicle side door: an experimental study for investigation of the force at the subjective pain threshold. J Biomech 2011; 44: 2158–2161.
[4] Hohendorff B, Weidermann C, Pollinger P, et al. Finger injuries caused by power-operated windows of motor vehicles: an experimental cadaver study. Injury 2012; 43: 903–907.
[5] Hohendorff B, Weidermann C, Pollinger P, Burkhart KJ, Prommersberger KJ, Müller LP. Einklemmung eines Kinder-fingers: Eine experimentelle Studie zur Bestimmung der elastischen Widerstände und der Punkte des Beginns der Knochen-/Gelenkdeformierung. Handchir Mikrochir Plast Chir 2012; 44: 1–4.
[6] Hohendorff B, Weidermann C, Pollinger P, et al. Verletzungsrisiko von Kinderfingern in automatischen Scheibenschließanlagen von Kraftfahrzeugen. Unfallchirurg 2012; 26 [Epub ahead of print], DOI: 10.1007/s00113-011-2150-3.
[7] Kent R, Stacey S, Parenteau C. Dynamic pinch tolerance of the phalanges and interphalangeal joints. Traffic Inj Prev. 2008; 9: 83–88.
[8] National Consumer Affairs Center of Japan. *NCAC News* 2010; Vol. 22 No. 3.
[9] National Highway Traffic Safety Administration. Federal motor vehicle safety standards and regulations, standard no. 118, power-operated window, partition, and roof panel systems. Title 49 of the Code of Federal Regulations, Part 571.118.
[10] National Highway Traffic Safety Administration, National Center for Statistics and Analysis. Not-in-traffic surveillance 2007 – highlights. DOT HS 811 085. 2009.
[11] Paridon HM, Mauser DM. Safeguarding of pinch and shear points on power windows by limitation of the closing velocity: a pilot study. Saf Sci 2006; 44: 197–207.